

# Experimental investigation of auto-ignition in non-premixed gaseous CH<sub>4</sub>/hot air cross flows

R. Dalshad<sup>1\*</sup>, T. Sander<sup>1</sup> and M. Pfitzner<sup>1</sup>

\*rahand.dalshad@unibw.de

<sup>1</sup> Institute for Thermodynamics, Department of Aerospace Engineering, Bundeswehr University Munich, Werner-Heisenberg-Weg 39, 85577 Neubiberg, Deutschland

## Abstract

In this work, an in-house test bench is introduced and first fundamental studies on auto-ignition delay are performed. Turbulent hot gas from fuel-lean combustion is redirected into a test section. Then, pure gaseous CH<sub>4</sub> at ambient pressure and temperature is injected perpendicularly to the turbulent hot flow from a jet nozzle integrated into a test plate. After the mixing of the flows and reaching stoichiometric conditions, ignition occurs. The ignition delay location is determined at different momentum ratios, which is a characteristic number for non-planar cooling films. To detect the chemical reaction, the chemiluminescence of hydroxyl radicals (OH) for the region of interest is recorded. OH is an intermediate product of the chemical reaction, therefore its concentration is used as an indicator for the start of the reaction (ignition delay). To calculate the initial conditions and model the test bench we use Cantera [1].

## Introduction

To achieve high thrust and efficiency, today's gas turbines and rocket chambers are operated at temperatures above the thermal resistance of common metals and alloys. Therefore, cooling of thermally stressed components is a non-negligible key element and state of the art. One of the most efficient cooling methods is film cooling. Here, cooling gas is injected to isolate and protect the surface from the main stream of the combustion chamber. But in fuel-rich operation of the combustion chambers or due to imperfect injection of fuel, the exhaust main flow contains residual unburnt fuel. The interaction between the hot main flow and the oxygen-rich cooling gas locally leads to stoichiometric conditions. With temperatures above the auto-ignition point of the fuels, chemical reactions may occur. Studies about such auto-ignition phenomena in oxygen-rich cooling films stabilized by fuel-rich hot gas are scarce in literature. Evans [2] was one of the first to visualize and investigate secondary combustion experimentally. He used a premixed well-stirred reactor (WSR) to produce the fuel-rich hot gas (propane) as main stream and redirected it to a mounted test section. Then, cold air was injected through different geometries into the main flow. Secondary reaction appeared between the two streams and a stable inverse diffusion flame was observed, which led to higher thermal loads to the wall. Later Blunck et al. [3] analyzed the flame structure of the same test rig based on chemiluminescence recordings. They confirmed that the blowing ratio affects the ignition location only slightly due to the change in penetration by the cooling gas. The ignition location as stated by Blunck is:

$$l = \frac{U_{cf}}{\tau} \quad (1)$$

where  $U_{cf}$  is the main flow (cross-flow) velocity and  $\tau$  the ignition delay time. The latter depends on temperature, pressure and chemistry, but not on the blowing ratio. Furthermore, flame instabilities resulted from turbulence of the main flow and from the tendency of inverse diffusion flames to be less stable than normal diffusion flames. OH-Planar laser induced fluorescence (OH-PLIF) results of fan shaped and normal jet cooling holes from Kostka et al. [4] showed flames anchored to the jet holes for normal injection, while for fan shaped holes reactions appeared downstream. In addition, peak OH intensity for normal holes is around a factor of two higher than for fan shaped hole. The enhanced reaction results from higher momentum of the normal jet perpendicular to the cross flow and better

mixing of the streams compared to the fan shaped case. Additionally, investigation of Richardson et al. [5] confirmed that cooling air separating from the wall lead to increased chemical reactions in normal direction, while attached films expand parallel to the wall. Results of CO-PLIF measurements indicate that CO is the driving component for secondary reactions to occur.

Other experimental literature of secondary reaction is hardly to find. Motivated by the need of more experimental data of this type of reactions and for validation purposes for in-house CFD codes, a new test bench is developed. First studies of fuel-lean cross-flow and cold methane ( $\text{CH}_4$ ) injection in normal direction is presented based on chemiluminescence images. The aims of this current set up is twofold:

- 1) Auto-ignition of methane in exhaust gas with oxygen fractions lower than air
- 2) Generating a stable secondary reaction zone and determining its position

Firstly, studies in literature specify the auto-ignition temperature range of methane. However, often the flow condition is unknown and the main flow is air. But the auto-ignition length depends amongst others on oxidizer availability and flow condition. In addition, alternative fuels such as hydrogen or propane can also be tested. Secondly, OH chemiluminescence images help to determine the fluctuation of the reaction zone. As stated before, the stability of the reaction zone depends on the cross-flow condition which we need to check for a new test bench. However, concluding from Blunck et al. [3] normal diffusion flames are more stable which should be beneficial for the current investigation. Further, determining the reaction position is necessary before performing measurements such as PLIF.

### Test bench and data acquisition

A new experimental setup is designed for reactive film cooling investigation. First part of the test bench is a purpose-designed reactor (burner) to generate hot exhaust gas as main stream. The burner is fed with fuel and oxidizer mixing inside the lower part of the burner, shown in Figure 1. The combustion chamber is equipped with temperature-resistant ceramics to improve the mixing of the reactants and has an effective volume of 2.47 l. Once ignited by a starter electrode, a steady reaction generates hot gas which enters the upper part separated by a flashback arrester. Then, the hot gas exits the burner from a cross section of around 50 mm x 50 mm.

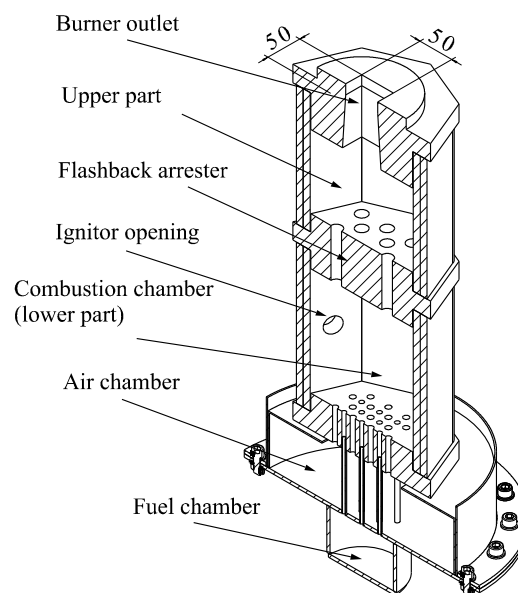


**Figure 1.** Sectional view of the burner interior

The second part is the test section mounted on top of the burner and connected to the exit, shown in Figure 2. The test section of the rig (50 mm x 50 mm) consists of a ceramic plate of 300 mm length and fused silica plates forming a rectangular duct providing optical access to the reaction zone. For the current chemiluminescence investigation only one side of the duct is equipped with quartz glass, steel plates cover the other two sides of the channel. A nozzle of 1.1 mm diameter is integrated into the ceramic plate 62.5 mm downstream the duct inlet and perpendicular to the main stream.

CH<sub>4</sub> and air are used as fuel and oxidizer for the burner. A considerable amount of fuel is necessary during the long operating times of the burner to reach high constant temperatures. Hence, 4 bottles (each 50 l, 200 bar) of CH<sub>4</sub> are interconnected and ensure an uninterrupted supply of fuel. The air is supplied by a reservoir fed by an in-house high-pressure compressor. Once desired exhaust gas conditions are achieved, pure CH<sub>4</sub> (cooling gas) at room temperature is injected through the nozzle. All the flows are regulated with Bronkhorst mass flow meters (burner CH<sub>4</sub>: F-113AC-1M0-RGD-44-V 300 l/min max.; burner air: F-203AV-1M0-RGD-44-V 1200 l/min max.; cooling/nozzle CH<sub>4</sub>: F-201AC-RAA-33-V 15 l/min max.) with the provider's control software.

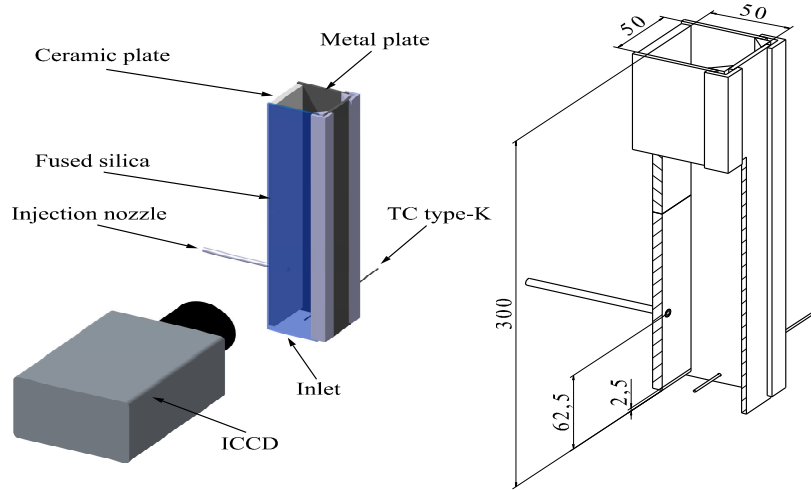


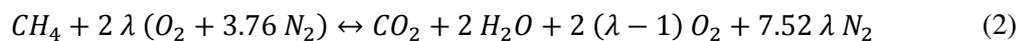
**Figure 2.** Test section and its sectional view. Dimensions in mm

Thermocouples (TC) of type-K are implemented in each gas supply line to measure the initial temperatures. A sheathed TC type-B is integrated inside the burner for monitoring the operation. Another TC type-K is installed inside the injection nozzle 10 mm before the cooling gas exits the ceramic plate. One more TC is necessary to measure the exhaust gas temperature before the interaction with the cooling gas. Therefore, a TC type-K of 1 mm diameter is located in the center of the inlet cross section, 2.5 mm downstream the ceramic plate. TC data acquisition was performed using a National Instruments cRio (9045) with a TC module and built-in calibration curves were applied to convert thermoelectric voltage into temperature.

Chemiluminescence images were recorded using a Princeton Instruments PI-MAX2 GEN ICCD camera. The camera was operated at 5 Hz, with an image resolution of 629 pixel x 1024 pixel and a magnification of 0.074 mm/pxl. The Nikon UV-Nikkor, 105 mm f/4.5, intensifier was set to maximum level and the aperture was fully open. From previous experiments, an exposure time of 500  $\mu$ s showed satisfying results at even low reaction rates. To reduce thermal emission and other reflection sources, a Chroma band-pass filter centered at 330 nm with a bandwidth of 40 nm was mounted in front of the lens. The filter provided a transmission of 55-60% of OH-emission in the relevant range from 308 nm to 314 nm. For each test condition, 200 single images were recorded, along with 50 pre- and 50 post-test background images where the nozzle injection was turned off. The amount of pictures is comparable to literature [3].

### Test conditions and post-processing

The investigation requires a high temperature and lean operation of the burner for oxygen-rich exhaust gas. The residual oxygen serves as oxidizer for the secondary reaction when cold CH<sub>4</sub> is injected through the nozzle and high temperatures are required for its auto-ignition. The global lean reaction for the CH<sub>4</sub> and air of the burner is given in Eq.(2).



where the air-fuel equivalence ratio is  $\lambda (>1)$ . We operated the burner at  $\lambda = 1.6$  which is a reasonable compromise between thermal condition ( $T_{ad} \approx 1700$  K) and oxygen content of the main stream. Further, the maximum temperature is limited to avoid damages to the burner.

For describing the interaction between main flow and cooling gas, different parameters exist, such as velocity ratio, blowing ratio and momentum ratio [6]. The injected cold  $CH_4$  from the nozzle is a three-dimensional jet penetrating the main stream and separates from the wall [7]. Therefore, we use the momentum ratio defined as:

$$I = \frac{\rho_c U_c^2}{\rho_h U_h^2} \quad (3)$$

where  $\rho$  is the density,  $U$  the velocity, and the subscripts  $c$  and  $h$  indicate the cooling gas and the hot main stream, respectively. During a test series, the main flow condition is kept constant, while the cooling gas velocity is increased to characterize the penetration depth, resulting in higher momentum ratio.

The TC at the inlet of the duct is exposed to temperatures above 1273 K, where heat loss due to radiation of its surface cannot be neglected. To account for the thermal loss and disregarding the emissivity of the surroundings, the convection-radiation energy balance for the TC can be expressed as follows [8]:

$$hA(T_h - T_{TC}) = \sigma A \varepsilon (T_{TC}^4 - T_\infty^4) \quad (4)$$

Since  $T_{TC}$  is measured directly, Eq.(4) can be rearranged for  $T_h$ :

$$T_h = \frac{\varepsilon \sigma}{h} (T_{TC}^4 - T_\infty^4) + T_{TC} \quad (5)$$

where  $T_\infty$  is the temperature of the surfaces emitting to the TC and assumed to be 300 K.  $\sigma$  is the Stefan-Boltzmann constant and  $\varepsilon$  is the emissivity of the TC.  $\varepsilon$  depends on parameters such as surface characteristics, oxidation etc. and experimental data are scarcely available for high temperature conditions. But at the same time, it has an enormous influence on the final corrected result. In literature [9]  $\varepsilon$  is specified as  $\sim 0.9$  (80 % Nickel, 20 % Chromium) at temperatures of 1273 K and 0.79 for non-oxidized Nichrome wire [10]. Therefore, we take  $\varepsilon = 0.8$  as recommended in [8]. Finally,  $h$  is the heat transfer coefficient calculated from the Nusselt correlation for spherical geometries as [11]:

$$Nu = 2 + \sqrt{Nu_{lam}^2 + Nu_{turb}^2} \quad (6)$$

with

$$Nu_{lam} = 0.664 \sqrt{Re_{d,TC}} \sqrt[3]{Pr_{d,TC}} \quad (7)$$

and

$$Nu_{turb} = \frac{0.037 Re_{d,TC}^{0.8} Pr_{d,TC}}{1 + 2.443 Re_{d,TC}^{-0.1} (Pr_{d,TC}^{2/3} - 1)} \quad (8)$$

$Re$  is the Reynolds number,  $Pr$  the Prandtl number and the subscript  $d$  indicates the diameter of the TC. Eq.(5) is solved iteratively, because the material properties are evaluated at the average temperature of  $T_{TC}$  and  $T_h$ .

In the current investigation, only volume flows are adjusted and temperatures are measured, other parameters such as flow and fluid properties have to be calculated. Hence, we perform equilibrium calculations with zero-dimensional reactors using Cantera [1]. Here, the burner is modelled as a non-reactive reactor to mix fuel and air, connected to a well-stirred reactor (WSR) and followed by a plug-flow reactor (PFR). The measured TC temperature is the input for the PFR and the heat loss due to radiation is corrected during the PFR process iteratively. Table 1 summarises the test conditions. The inlet TC temperature is corrected for radiation losses. The Reynolds number is based on the hydraulic diameter of the burner and  $U_h$  is the average main stream velocity without boundary layer effects. Both are averaged over the three momentum ratios for constant  $CH_4$ . We increased the cooling gas flow gradually resulting in different momentum ratios. Further, the molar composition of the exhaust gas is almost constant for the main components due to constant  $\lambda$  and similar temperatures. From Cantera we get molar fractions of  $x_{O_2} = 7.4\%$ ,  $x_{N_2} = 74\%$ ,  $x_{CO_2} = 6.2\%$ ,  $x_{H_2O} = 12.3\%$ ,  $x_{OH} = 1e^{-2}$  to  $2.3e^{-2}\%$ . Compared to air, the fraction of oxygen is three times less.

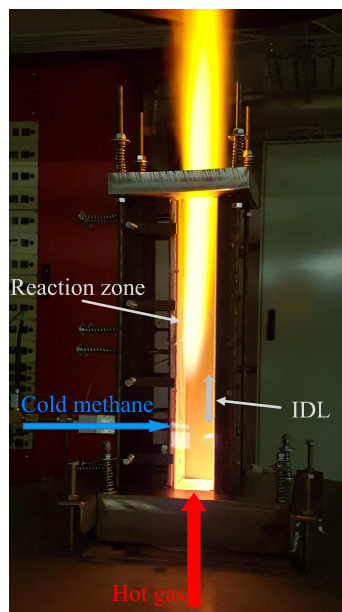
**Table 1.** Experimental conditions

| Burner $CH_4$ in l/min | $T_{TC}$ in K             | Average $Re_{a,h}$ | Average $U_h$ in m/s | I                      |
|------------------------|---------------------------|--------------------|----------------------|------------------------|
| 30                     | 1537 ; 1549 ; 1559        | 3603               | 18                   | 3.8 ; 14.8 ; 32.7      |
| 35                     | 1577 ; 1581 ; 1590        | 4145               | 21                   | 3.8 ; 15.1 ; 33.5      |
| 40                     | 1599 ; 1611 ; 1618        | 4685               | 25                   | 4.01 ; 16.01 ; 35.7    |
| 45                     | 1648 ; 1653 ; 1654 ; 1654 | 5173               | 28                   | 3.9 ; 15.3 ; 34.5 ; 61 |

Before evaluating the camera images some basic post-processing was necessary. First, applying Matlab's 'imnlmfilt', a non-local means-based filter [12], to each experiment image helped to reduce the noise. Then, a simple averaging of the background images was performed, in order to subtract the background from the experimental images. Later, the processed experimental images were averaged.

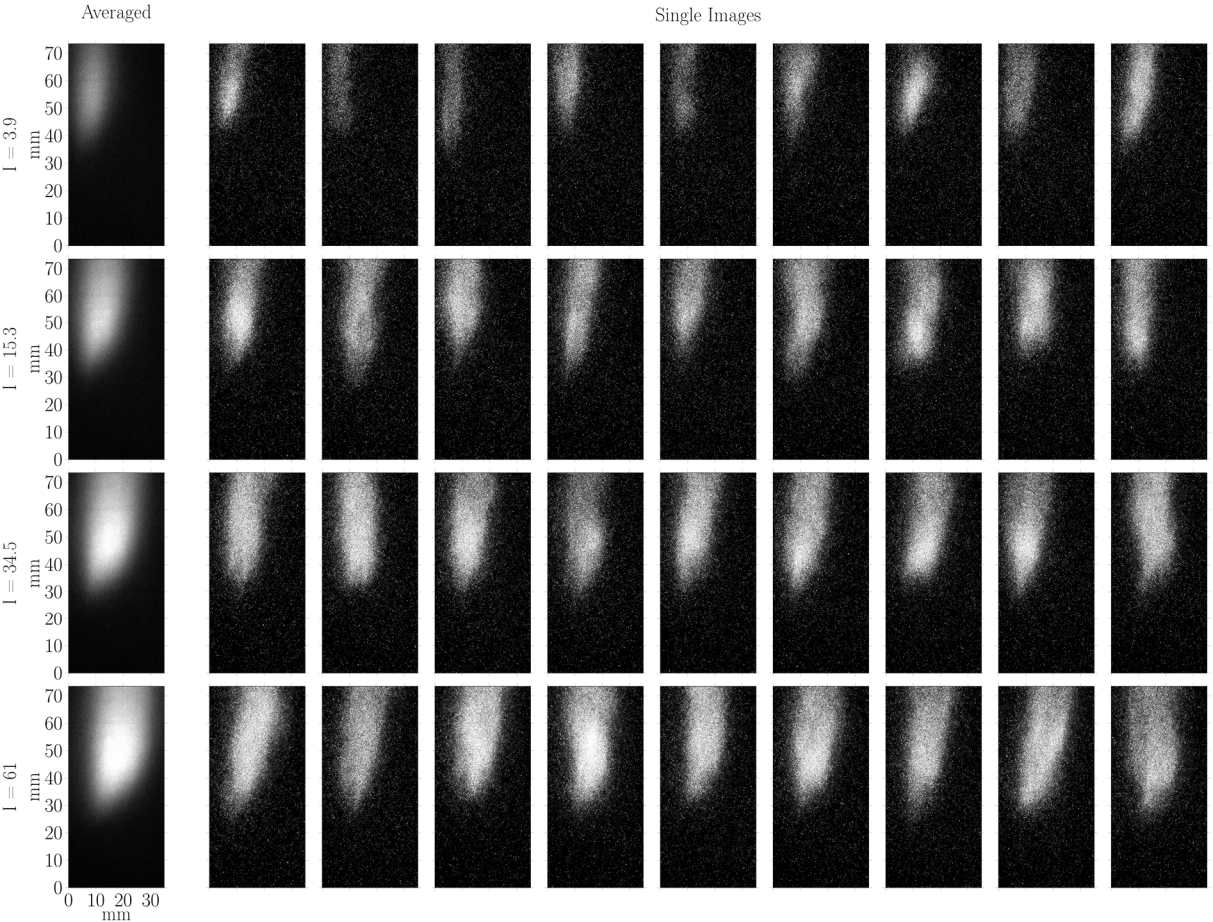
### Results and discussion

Figure 1 illustrates the setup during an experiment with a high volume rate of cold  $CH_4$ . Hot gas of the burner enters from the bottom cross-section and cold  $CH_4$  is injected perpendicular inside the test section. After an ignition delay length (IDL), where mixing of  $CH_4$  and hot gas takes place, a bright reaction zone occurs and broadens downstream. Due to the high amount of  $CH_4$  the reaction extends to some distance after the test section exit. The reaction zone inside the test section is subject of investigation and characterization based on chemiluminescence images.



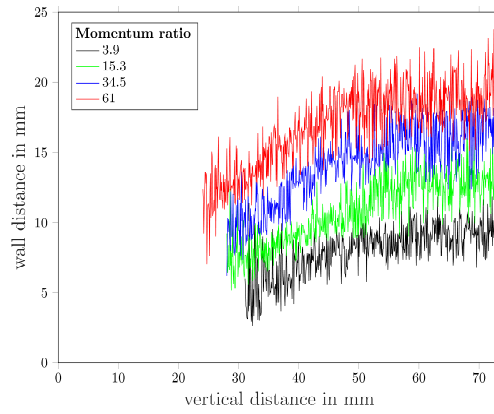
**Figure 3.** Experimental setup

Figure 4 shows 9 single images recorded successively and one averaged (left) over 200 images. The main flow condition is constant and all images are at the same intensity level for a better comparability. The main flow enters from bottom and the injection of the cooling gas is located in (0,0), see scale on the left bottom corner in Figure 4. Higher momentum ratios  $I$  clearly lead to enhanced reactions, as seen from the intensities. The intensity maxima increase and the reaction zone expands. According to the single images, the diffusion flame stays at an almost constant at horizontal and vertical position. The standard deviation of the vertical position is 6.5 % to 11 % of the mean vertical location. The calculation is based on the location where the intensity increases by 50 % of the maximum. The fluctuations are lowest for the highest momentum ratio and for the highest main flow velocity. Increasing the momentum ratio stabilizes the jet and the secondary combustion. Also, increasing the burner output results in higher main flow temperatures (Table 1) but also in a more homogeneous flow. In comparison, Blunck [3] reported standard deviation of the flame tip location from 25 % to 35 % of inverse diffusion flames and angled slot injection. However, the definition of the flame tip or flame front is not specified. Due to the small fluctuations, the number of images for averaging is adequate.



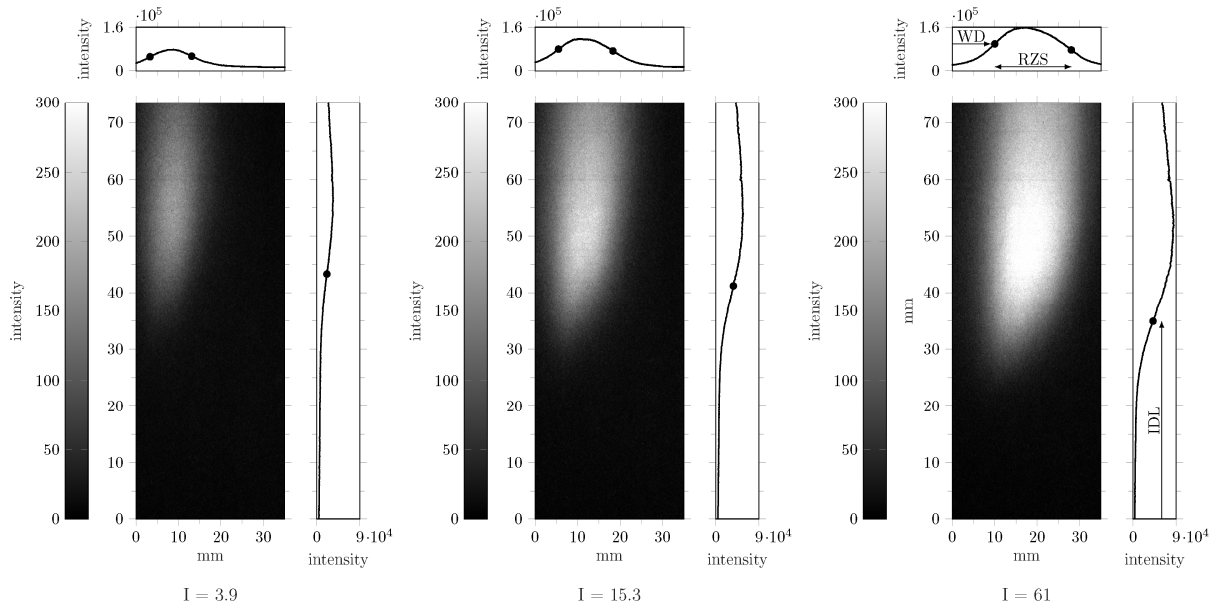
**Figure 4.** Averaged and single images of OH chemiluminescence for  $U_h=28$  m/s

Figure 5 shows the horizontal position of maximum OH chemiluminescence plotted over the vertical distance for the averaged images. Increasing the momentum ratio causes the wall distance to increase by approximately 100 % from  $I = 3.9$  to  $I = 61$ . For constant momentum ratios, higher separation downstream the injection nozzle is also observed.



**Figure 5.** OH intensity peaks of wall distance vs. vertical downstream position for  $U_h = 28$  m/s

A possibility to compare the average images of different main flow conditions quantitatively is demonstrated in Figure 6. Adding together all pixel intensities over the horizontal and the vertical axis yields the intensity distribution curves on the top and on the left of each image in Figure 6.



**Figure 6.** Intensity curves for different momentum ratios for  $U_h = 28$  m/s and definition of wall distance (WD), reaction zone size (RZS) and ignition delay length (IDL) on right

Now, different methods can be applied to determine the flame front, such as intensity rise of an arbitrarily defined limit. For this intercomparison study we decided for the location of the inflexion point of the intensity curves. Therefore, the intensity distribution was approximated by a polynomial fitting function using Matlab. Then, the location of the inflexion point of the right curve is defined as the IDL, the location of the first inflexion point of the top curve is the wall distance (WD), while the distance to the next inflexion point on this curve is considered as the reaction zone size (RZS). This definition is only valid for the current investigation, because the measurement is not based on quantitative OH emission. The inflexion points as well as the location of intensity maxima depend on the momentum ratio. Furthermore, an ignition delay length is observed for the diffusion flames compared to Kostka et al. [4] where anchored inverse diffusion flames occurred for normal injection. However, they used propane as fuel, whereas we use methane. Propane has a lower auto ignition temperature and lower flammability limit than methane. Figure 7 summarises the results for all test cases from Table 1. The IDL for the main flow velocities from 18 m/s to 25 m/s are similar. But the deviation of the IDL at 28 m/s amounts to approximately 10 % to 16 %. This can be a consequence of the main flow temperature and more stable main flow condition. The WD shows the highest variation at the lowest momentum

ratio because by increasing momentum ratio the flame reaction zone stabilizes. On the other hand, the spreading in RZS is constant over the momentum ratio.

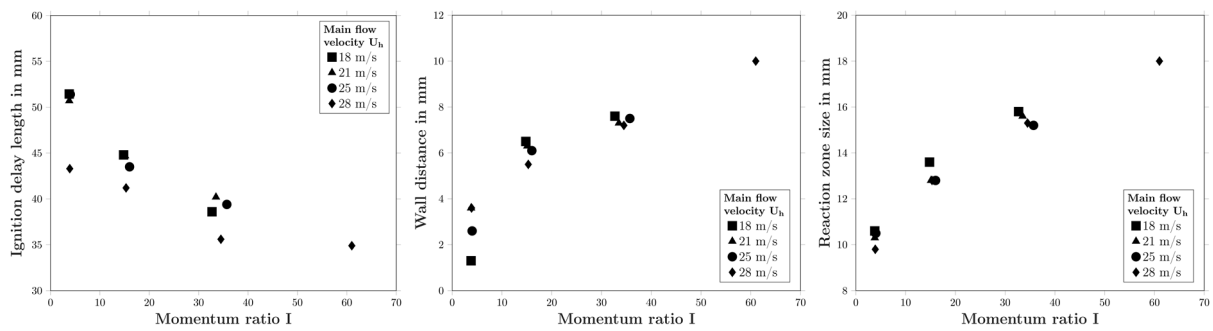


**Figure 7.** IDL, WD and RZS plotted against I

The single images as well as the quantifications based on IDL, WD and RZS reflect the comparability of the different test conditions. Furthermore, fluid-mechanical phenomena such as wall separation due to high momentum flux and reactive flows are observed and visualized.

### Summary and conclusion

A new test bench is designed for reactive film cooling investigation. Oxygen-rich exhaust gas was generated from the lean combustion of methane. The hot gas was introduced to a test section where cold methane was injected through a nozzle perpendicularly. After the mixing of cold and hot gas secondary ignition was observed. The test section was equipped with fused silica that enabled optical access to the reaction zone. OH-chemiluminescence was recorded at 5 Hz using an ICCD and a optical filter. The images helped to determine reaction parameters optically. Thermocouple data were radiation-convection corrected and unknown flow parameters were calculated with Cantera.

The investigation showed that a mixture of methane and hot exhaust gas leads to auto-ignition. Here, main flow velocities up to 28 m/s and momentum ratios from 3.8 to 61 were tested. OH-chemiluminescence of the reaction zone region was recorded successfully. The single images showed minor fluctuations and a stable reaction zone (11 % standard variation of vertical position), consequently 200 images were sufficient for averaging. Then, the intensities were summed up in vertical and horizontal direction to determine ignition delay length, wall distance and the size of the reaction zone based on the inflexion point. Increasing the momentum ratio, led to an enhanced reaction zone and increased the wall separation of the reaction zone due to high momentum flux. In contrast to experimental data from Kostka et al. [4], where propane was tested, the secondary reaction from normal injection of methane showed an ignition delay length instead of an anchored flame to the nozzle. The results for constant momentum ratio and varied main flow velocity were in good agreement (maximum deviation of 16 %). Despite the fact that the ignition location is independent of the blowing ratio and momentum ratio, we observed a reduction of the reaction length with increasing momentum ratio.

### Future work

The aims of future investigations are the implementation of different geometries, measuring the wall heat flux resulting from the reaction zone and applying OH-PLIF. The test bench is designed in a modular manner. The test section can be modified or replaced completely. In future experiments a water cooled flat plate will be installed for defined thermal boundary conditions. Furthermore, since the wall heat flux is a parameter of interest, it needs to be determined for thermal analysis and for our in-house CFD codes. In addition, OH-PLIF will be applied for quantitative optical measurements of the reaction zone. Using our laser systems we can perform qualitative OH measurements as well as temperature measurements based on two or multi line excitation.

### Acknowledgment

The authors gratefully acknowledge Issendorff Thermoprozesstechnik e.K. for the design and production of the burner.

## Literatur

- [1] "Cantera," [Online]. Available: <https://cantera.org/>. [Accessed 2019].
- [2] D. S. Evans, "The Impact of Heat Release in Turbine Film Cooling," Thesis, Wright-Patterson Air Force Base, Ohio, 2008.
- [3] D. Blunck, S. Kostka, A. Lynch, M. Polanka, S. Stouffer, S. Roy, J. Zelina und J. R. Gord, „Flame Structure of Vitiated Fuel-rich Inverse Diffusion Flames in Cross-Flow,“ in *th US National Combustion Meeting Organizes by the Eastern States Section of the Combustion Institute and Hosted by the Georgia Institute of Technology, March 20-23, 2011*, Atlanta, GA, 2011.
- [4] S. Kostka, D. Blunck, N. Jiang, A. Lynch, M. Polanka, S. Stouffer, R. J. Gord und S. Roy, „Temperature on Inverse Diffusion Flames in a Vitiated Cross-Flow using Two-Color PLIF Thermometry,“ in *Fall Technical Meeting of Eastern States Section of the Combustion Institute Hosted by the University of Connecticut, Storres, CT*, 2011.
- [5] D. R. Richardson, N. Jiang, D. L. Blunck, J. R. Gord und S. Roy, „Characterization of inverse diffusion flames in vitiated cross flows via two-photon planar laser-induced fluorescence of CO and 2-D thermometry,“ *Combustion and Flame* 168, Bd. 168, pp. 270-285, 2016.
- [6] R. Dalshad, M. Straußwald, T. Sander und M. Pfitzner, „Isothermal PIV Measurement of Planar Film Injection with Regard to Reactive Film Cooling,“ in *5th International Conference on Experimental Fluid Methanics ICEFM 2018*, Munich, Germany, 2018.
- [7] J. R. Goldstein, "Film Cooling," *Advances in Heat Transfer, Vol. 7*, pp. pp. 321-379, 1971.
- [8] I. Roberts, J. Coney und B. Gibbs, „Estimation of radiation losses from sheathed thermocouples,“ *Applied Thermal Engineering* 31, pp. 2262-2270, 2011.
- [9] Y. Touloukian und D. DeWitt, *Thermal Radiative Properties - Metallic Elements and Alloys*, New Yourk: Springer Science+Business Media, 1970.
- [10] MIKRON, "TABLE OF EMISSIVITY OF VARIOUSSURFACES," [Online]. Available: [http://www-eng.lbl.gov/~dw/projects/DW4229\\_LHC\\_detector\\_analysis/calculations/emissivity2.pdf](http://www-eng.lbl.gov/~dw/projects/DW4229_LHC_detector_analysis/calculations/emissivity2.pdf). [Accessed 31 05 2019].
- [11] Verein Deutscher Ingenieure e.V., *VDI-Wärmeatlas*, Heidelberg: Springer-Verlag Berlin, 2013.
- [12] Mathworks, "Documentation imnlmfil," [Online]. Available: <https://de.mathworks.com/help/images/ref/imnlmfil.html>. [Accessed 04 2019].
- [13] D. J. Micka und J. F. Driscoll, „Stratified jet flames in heated (1390 K) air cross-flow with autoignition,“ *Combustion and Flame* 159, pp. 1205-1214, 2012.